



eROSITA

P. Predehl on behalf of the eROSITA Team

Max-Planck-Institut für extraterrestrische Physik – Giessenbachstrasse, D-85748 Garching, Germany, e-mail: predehl@mpe.mpg.de

Abstract. eROSITA (extended ROentgen Survey with an Imaging Telescope Array) is the core instrument on the Russian Spektrum-Roentgen-Gamma (SRG) mission which is currently scheduled for launch in 2014. eROSITA will perform a deep survey of the entire X-ray sky. In the soft band (0.5-2 keV), it will be about 30 times more sensitive than ROSAT, while in the hard band (2-8 keV) it will provide the first ever true imaging survey of the sky. The design driving science is the detection of large samples of galaxy clusters out to redshifts $z > 1$ in order to study the large scale structure in the Universe and test cosmological models including Dark Energy. In addition, eROSITA is expected to yield a sample of a few million AGN, including obscured objects. The survey will also provide new insights into a wide range of astrophysical phenomena, including X-ray binaries, active stars and diffuse emission within the Galaxy. eROSITA is currently in its qualification phase. The first of seven flight mirror modules (+ 1 spare) has been delivered.

Key words. X-rays: all-sky surveys: Cosmology: large scale structure

1. Introduction

The Russian Spektrum-Roentgen-Gamma (SRG) mission is based on a medium class platform ("Navigator", Lavochkin Association, Russia). The launch will be in 2014 using a Zenith-Fregat rocket from Baikonur into an orbit around the Langrangian Point L2. The payload consists of the X-ray instruments eROSITA (= extended ROentgen Survey with an Imaging Telescope Array) and ART-XC (= Astronomical Roentgen Telescope - X-ray Concentrator).

eROSITA is currently being built, assembled and tested under the leadership of the Max-Planck Institute for Extraterrestrial Physics (MPE). In the first four years of scientific operation, eROSITA will perform a deep survey of the entire X-ray sky. In the soft X-ray

band (0.5-2 keV), this will be about 30 times more sensitive than the ROSAT all sky survey, while in the hard band (2-8 keV) it will provide the first ever true imaging survey of the sky at those energies. Such a sensitive all-sky survey will revolutionise our view of the high-energy sky, and calls for major efforts in synergic, multi-wavelength wide area surveys in order to fully exploit the scientific potential of the X-ray data. The all-sky survey program will be followed by 3 years of pointed observations, with open access through regular announcement of opportunities for the entire astrophysical community. With on-axis spatial resolution comparable to XMM-Newton, and a larger effective area at low energies, eROSITA will provide a powerful and highly competitive X-ray observatory for the next decade.

The seven eROSITA telescopes are extended versions of the existing ABRIXAS de-

sign (effective area increased by a factor of five) plus an advanced version of the pnCCD camera successfully flying on XMM-Newton (increased Field of View by a factor of two).

Similar to eROSITA, ART-XC contains 7 telescopes working in the energy range between 6 and 30 keV. The telescopes have CdTe detectors in their focal planes (Pavlin et al. 2013).

2. Scientific goals

The design-driving science of eROSITA is the detection of very large samples ($\approx 10^5$ objects) of galaxy clusters out to redshifts $z > 1$, in order to study the large scale structure in the Universe, test and characterize cosmological models including Dark Energy.

The galaxy cluster population provides information on the cosmological parameters in several complementary ways:

1. The cluster mass function in the local Universe mainly depends on the matter density Ω_m and the amplitude of the primordial power spectrum σ_8 .
2. The evolution of the mass function $f(M, z)$ is directly determined by the growth of structure in the Universe and therefore gives sensitive constraints on Dark Matter and Dark Energy.
3. The amplitude and shape of the cluster power spectrum, $P(k)$ and its growth with time depend sensitively on Dark Matter and Dark Energy.
4. Baryonic wiggles due to the acoustic oscillations at the time of recombination are still imprinted on the large scale distribution of clusters and thus can give tight constraints on the curvature of space at different epochs.

eROSITA is also expected to yield a sample of around 3 million Active Galactic Nuclei, including both obscured and unobscured objects, providing a unique view of the evolution of supermassive black holes within the emerging cosmic structure. The survey will also provide new insights into a wide range of astrophysical phenomena, including accreting binaries,

active stars and diffuse emission within the Galaxy, as well as studies of solar system bodies that emit X-rays via the charge exchange process. Moreover, such a deep imaging survey at high spectral resolution, with its scanning strategy sensitive to a range of variability timescales from tens of seconds to years, will undoubtedly open up a vast discovery space for the study of rare, unpredicted, or unpredictable high-energy astrophysical phenomena.

3. Instrument

A schematic view of eROSITA is seen in figure 1 (see also Predehl 2012). The optical bench consists of a system of carbon fibre honeycomb panels connecting the mirror modules and the baffles on one side with the focal plane instrumentation on the other side. A hexapod structure forms the mechanical interface to the S/C bus.

Seven single mirror modules are arranged in a hexagonal shape. Each of the modules comprises 54 paraboloid / hyperboloid mirror shells (Wolter-I geometry) with an outer diameter of 360 mm and a common focal length of 1.600 mm. The on-axis resolution of all mirror modules shall be within 15 arcsec HEW at 1.5 keV (Friedrich et al. 2012). The geometry of a Wolter-I mirror system cannot prevent that photons from X-ray sources outside the field of view reach the camera by single reflection on the hyperboloid. These unwanted photons increase the background and can be suppressed only by an "X-ray baffle" in front of the mirror module. The baffles consist of 54 concentric invar-cylinders mounted on spider wheels, thereby precisely matching the footprint of the parabola entrance of each mirror shell. Magnetic electron deflectors behind the mirrors help in reducing background due to low energy cosmic-ray electrons.

Each mirror system has a CCD camera in its focus. The eROSITA-CCDs have 384 x 384 pixels on an image area of 28.8 mm x 28.8mm, respectively, for a field of view of 1.03° diameter. The 384 channels are read out in parallel using special ASICs ("CAMEX"). The nominal integration time for eROSITA is 50 msec (Meidinger et al. 2011). The CCDs are pro-

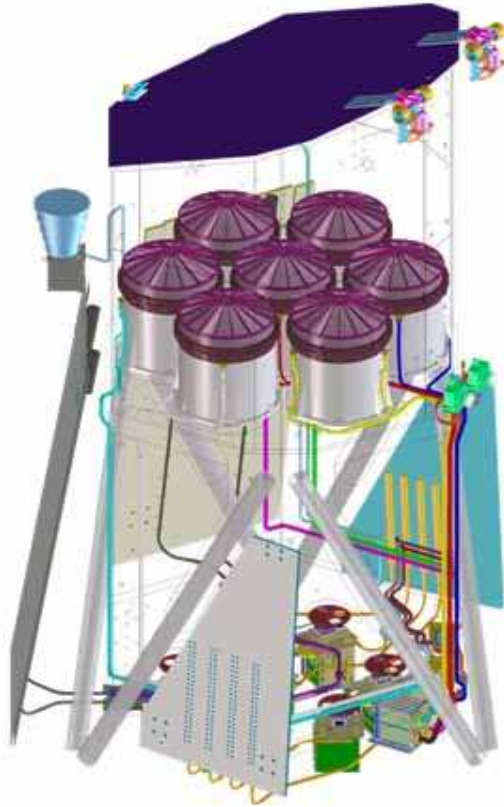


Fig. 1. Schematic drawing of the telescope with the seven identical telescopes = mirrors with baffles on top (magenta), cameras with filterwheels and E-boxes at bottom, front cover (dark blue), star- (cyan) and sunsensors (green) and the four radiators (grey), two for the cooling of the cameras, two smaller ones for the cooling of the electronics. The optical bench is only adumbrated.

tected from proton radiation by means of a massive copper shielding. Fluorescence X-ray radiation generated by cosmic particles is minimized by a graded shield consisting of aluminium, beryllium and boron-carbide. For calibration purposes, each camera has its own filterwheel with a radioactive Fe^{55} source and an aluminium target providing two spectral lines at 5.9 keV ($\text{Mn-K}\alpha$) and 1.5 keV ($\text{Al-K}\alpha$). For operation the CCDs have to be cooled down to -90°C by means of passive elements (heat pipes and radiators).

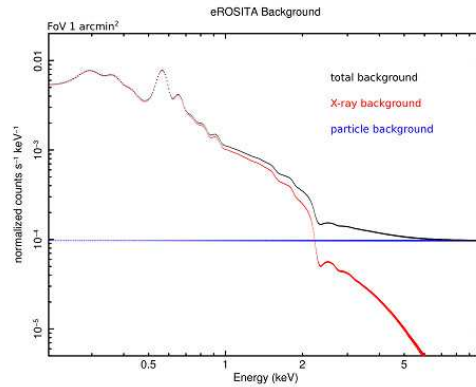


Fig. 2. Simulated (XSPEC) eROSITA background (black) and spectral components: in red the photon X-ray background (galactic and extragalactic), in blue the particle background and in black the total.

Two (redundant) startrackers are mounted on eROSITA for accurate boresighting. The dimensions of the telescope structure is approximately 1.9 m diameter x 3.2 m height. The total weight of eROSITA is 810 kg.

3.1. Sensitivity

The expected eROSITA background (figure 2) has been simulated based on photon and high-energy particle spectral components. The cosmic diffuse photon X-ray background has been adopted from the measurements with the XMM-Newton EPIC cameras, as reported in Lumb et al. (2002). The high-energy particle background has been calculated with Geant4 simulations by Tenzer et al. (2010) (see also Perinati et al. 2012). The expected background count rate has been compared with XMM-Newton observations, which might provide the best test for the photon background for eROSITA around the Lagrangian point L2 before real photon background data will become available.

For the point source sensitivity (Merloni et al. 2012) we have assumed an extraction region of $60''$ diameter ($2\times\text{HEW}$ averaged over the FoV), and a background count rate of $7.70\text{ cts s}^{-1}\text{deg}^{-2}$ and $3.31\text{ cts s}^{-1}\text{deg}^{-2}$ in the soft and hard band, respectively, and requiring

a false detection probability $P_{null} < 2.87 \times 10^{-7}$ (i.e. the Gaussian upper-tail probability for 5σ). The PSF characterisation of the eROSITA telescope suggests that about 20% of the total point sources flux is expected to lie outside the $60''$ diameter extraction region, thus a 1.2 multiplicative correction factor has been applied. The overall flux limits in the two bands are then finally computed by multiplying the count rates by the appropriate conversion factors, calculated assuming a power-law spectrum with photon index $\Gamma = 1.8$ and column density $N_H = 3 \times 10^{20} \text{ cm}^{-2}$. These are given by 1.42×10^{-12} and $2.81 \times 10^{-11} \text{ erg}^{-\text{s}} \text{ cm}^{-2} / \text{count rate}$ for the soft (0.5-2 keV) and hard (2-10 keV) bands, respectively. The bottom panel of figure 3 shows the predicted sensitivity as a function of exposure time for both the soft and hard bands. For point sources, we first estimated the total net counts needed to securely identify a point source as a function of exposure time (top panel of figure 3). We did this by estimating the full Poisson probability of spurious detection (P_{null}), given the number of background (nB) and total detected counts (nT) (Weisskopf et al. 2007).

For extended sources, the source detection process is more complicated and depends in detail on the source properties. The most numerous and important set of extended sources in the eROSITA survey are galaxy clusters, which are generally characterised by a compact appearance of the source with a bright central region and a steep decline of the surface brightness to larger radii, which can be described with some approximation by a beta-model (Cavaliere & Fusco-Femiano 1976). We have made simulations of the eROSITA sky area of about $1.9 \times 1.2 \text{ sqdeg}$ in size, with exposures of 2.2 ks (approximately at the average exposure of the all sky survey) and 30 ks (\approx deepest exposure in the ecliptic pole region) from Mühlegger (2011). The most prominent extended cluster sources are easily noted in figure 5. The detection threshold for extended sources has to be determined from detailed simulations, possibly including realistic structural properties of clusters, such as cool-cores and disturbed morphologies, as well as the evolution of their incidence as a function of cosmic

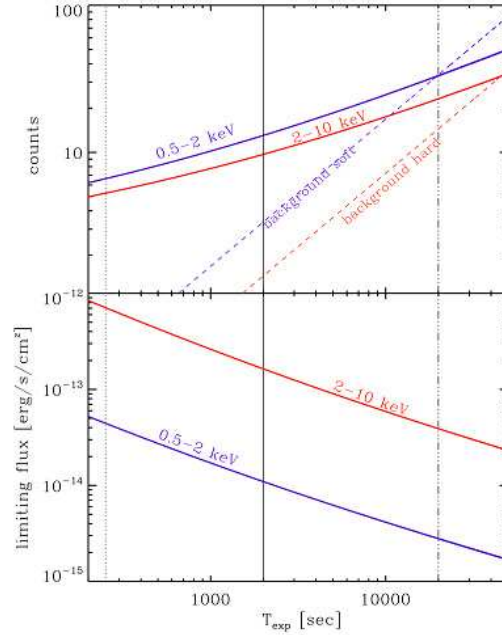


Fig. 3. Top panel: Minimum number of net counts needed to securely identify a point source in survey mode (HEW $30''$) as a function of exposure time for soft (0.5-2 keV, blue solid line) and hard (2-10 keV, red solid line) band respectively. The corresponding dashed lines are the expected number of background counts in a $1'$ diameter extraction region. Bottom: Sensitivity plot for AGN (power-law with photon index $\Gamma = 1.8$ and $N_H = 3 \times 10^{20}$), e.g. point sources limiting flux versus exposure time. Three vertical lines are shown, marking the average exposure times for one all-sky survey (eRASS:1, 6 months; 250 s, dotted), the final 4-years all-sky survey (eRASS:8, 2 ks, solid) and the 4-years deep exposure at the ecliptic poles (20 ks, dot-dashed), where a survey efficiency of 80% has been assumed.

time. Here we present, as an illustration, simple estimates based on analytic calculations which accounts for all known expected instrumental effects. There are two types of thresholds that are of interest for our purpose: the detection threshold as an X-ray source and the threshold for characterising the source as clearly extended. For the detection threshold, we compute this again using the full bimodal probability (see above), computed for a 0.5-2 keV background within an extraction region of 3

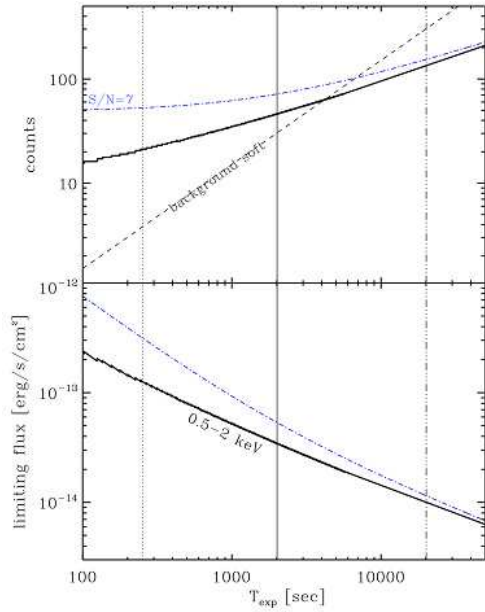


Fig. 4. Top panel: Minimum number of net counts needed to securely identify an extended source in survey mode as a function of exposure time in the 0.5-2 keV band. Thick solid line is for Poissonian probability threshold, while dot-dashed line marks a fixed $S/N=7$ (see text for details). The corresponding dashed lines are the expected number of background counts in a 3' diameter extraction region. Bottom: Sensitivity plot for clusters (APEC model in XSPEC assumed at $z=0.2$) with $T = 2$ keV, metallicity of 0.3 solar and $N_H = 3 \times 10^{20}$). Three vertical lines are shown, marking the average exposure times for one all-sky survey (eRASS:1, 6 months; 250 s, dotted) the final 4-years all-sky survey (eRASS:8, 2 ks, solid) and the 4-years deep exposure at the ecliptic poles (20 ks, triple-dot-dashed).

arcmin diameter. In analogy with the point-source case, in figure 4 we show both the net counts (top panel) and the limiting 0.5-2 keV flux (bottom panel) as a function of exposure time. In this case, however, we have set a more stringent limit for spurious detection ($P_{null} < 2.56 \times 10^{-12}$ i.e. the Gaussian upper-tail probability for 7σ). For a rough estimate of how such a threshold needs to be raised when we seek for a characterization of the detected sources, we plot in the same figure (dotdashed lines) the limiting flux and net counts obtained by requir-

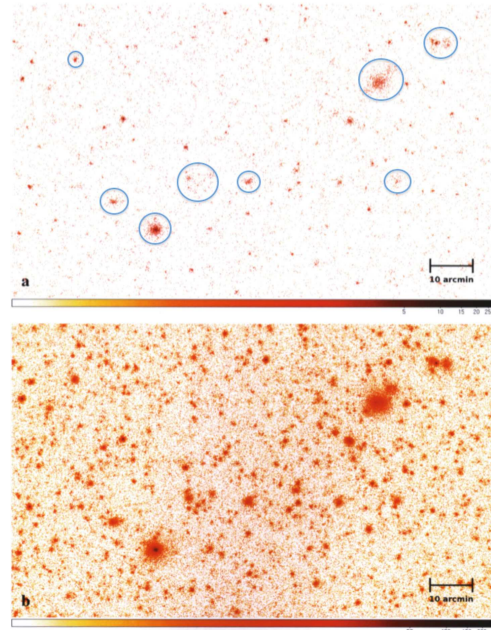


Fig. 5. Simulated region of the eROSITA survey including point sources, extended cluster sources, and diffuse background. The upper panel shows a region of $1.9 \times 1.2 \text{ deg}^2$ as would be observed in the main survey with an exposure of 2.2 ks, while the lower panel shows the same region as would be observed at the ecliptic poles with an exposure of 30 ks (from Mühlegger 2011). Extended structures are highlighted in the top panel.

ing a minimal signal-to-noise ratio $S/N = 7$, where $S/N = \sqrt{nS/(nT)}$ with nS denoting the net (source) and nT the total (source plus background) counts, respectively.

4. Status

eROSITA is currently in its qualification phase (figure 6): The whole instrument just underwent all the qualification tests, i.e. vibration, acoustic noise, thermal vacuum (or "space simulation" including sunlight, respectively) successfully. The first flight mirror module (FM-1) is delivered and tested in our long-beam test facility PANTER. It turns out to be completely within the specification with respect to angular resolution and effective area. All CCDs are fabricated and tested, the rather complicated elec-



Fig. 6. The eROSITA qualification model on the shaker for vibration tests

tronics (9 boxes, 61 printed circuit boards) is in the test phase.

Acknowledgements. eROSITA is funded equally by the Deutsches Zentrum für Luft und Raumfahrt (DLR) and the Max-Planck-Gesellschaft zur Förderung der Wissenschaften (MPG).

References

- Burwitz, V., Friedrich, P., Bräuninger, H., et al. 2011, SPIE, 8147, 08
 Cavaliere & Fusco-Femiano, F. 1976, A&A, 49, 137
 Friedrich, P., Bräuninger, H., Budau, B., et al. 2012, SPIE, 8443, 1S
 Fürmetz, M., Predehl, P., Eder, J., Tiedemann, L. 2010, SPIE, 7732, 3K
 Lumb, D.H., Warwick, R.S., Page, M., De Luca, A. 2002, A&A, 389, 93
 Meidinger, N., Andritschke, R., Elbs, J., et al. 2011, SPIE, 8145, 02
 Merloni et al.: "The eROSITA Science Book", 2012, arXiv1209.3114M
 Mühlegger, 2011, Ph.D. thesis, TU München
 Pavlinsky, M., et al.: 2013, this conference
 Perinati, E., Tenzer, c., Santangelo, A., et al., 2012, Experimental Astronomy, 33, 39
 Predehl, P. 2012, SPIE, 8443, 1R
 Tenzer, C., Warth, G., Kendziorra, E., Santangelo, A. 2010, SPIE, 7742, 0Y
 Weisskopf, M.C., Wu, K., Trimble, V., et al., 2007, ApJ, 657, 1026